YMTHE, Volume *25*

Supplemental Information

Rescue of Hearing by Gene Delivery to Inner-Ear Hair Cells Using Exosome-Associated AAV

Bence György, Cyrille Sage, Artur A. Indzhykulian, Deborah I. Scheffer, Alain R. Brisson, Sisareuth Tan, Xudong Wu, Adrienn Volak, Dakai Mu, Panos I. Tamvakologos, Yaqiao Li, Zachary Fitzpatrick, Maria Ericsson, Xandra O. Breakefield, David P. Corey, and Casey A. Maguire

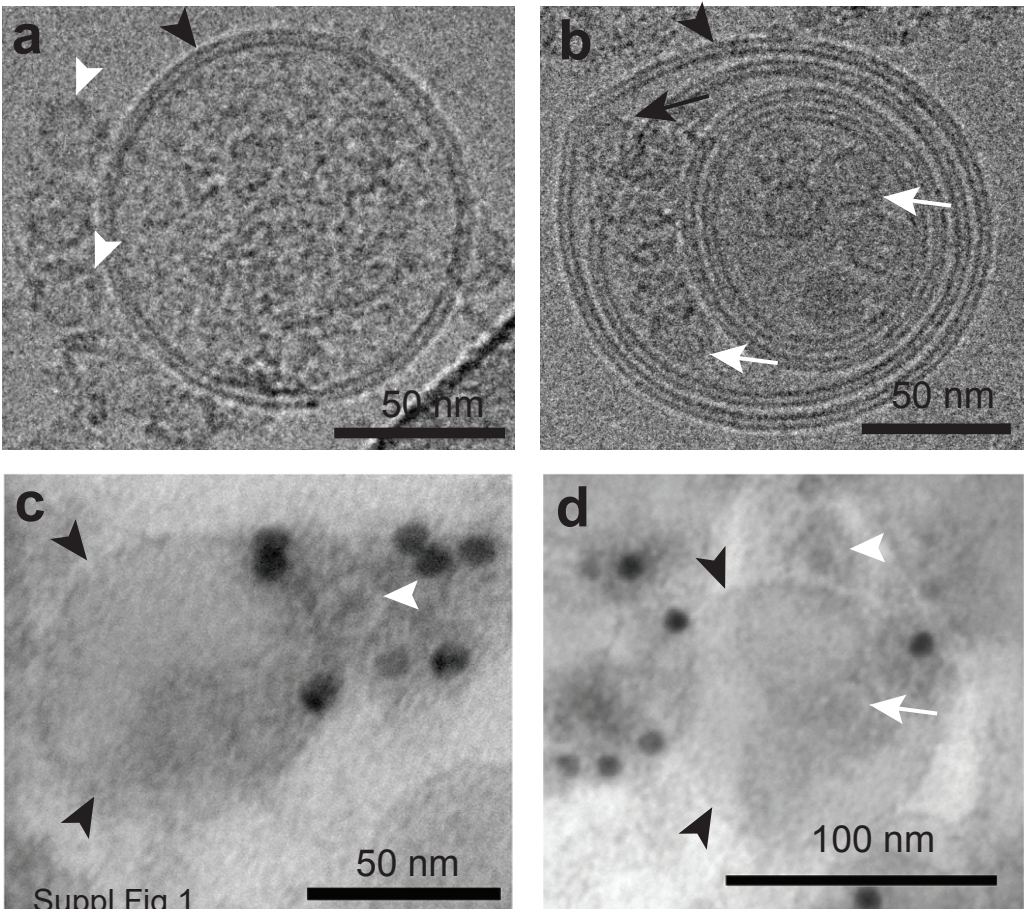

Suppl Fig 1

Suppl. Fig 2

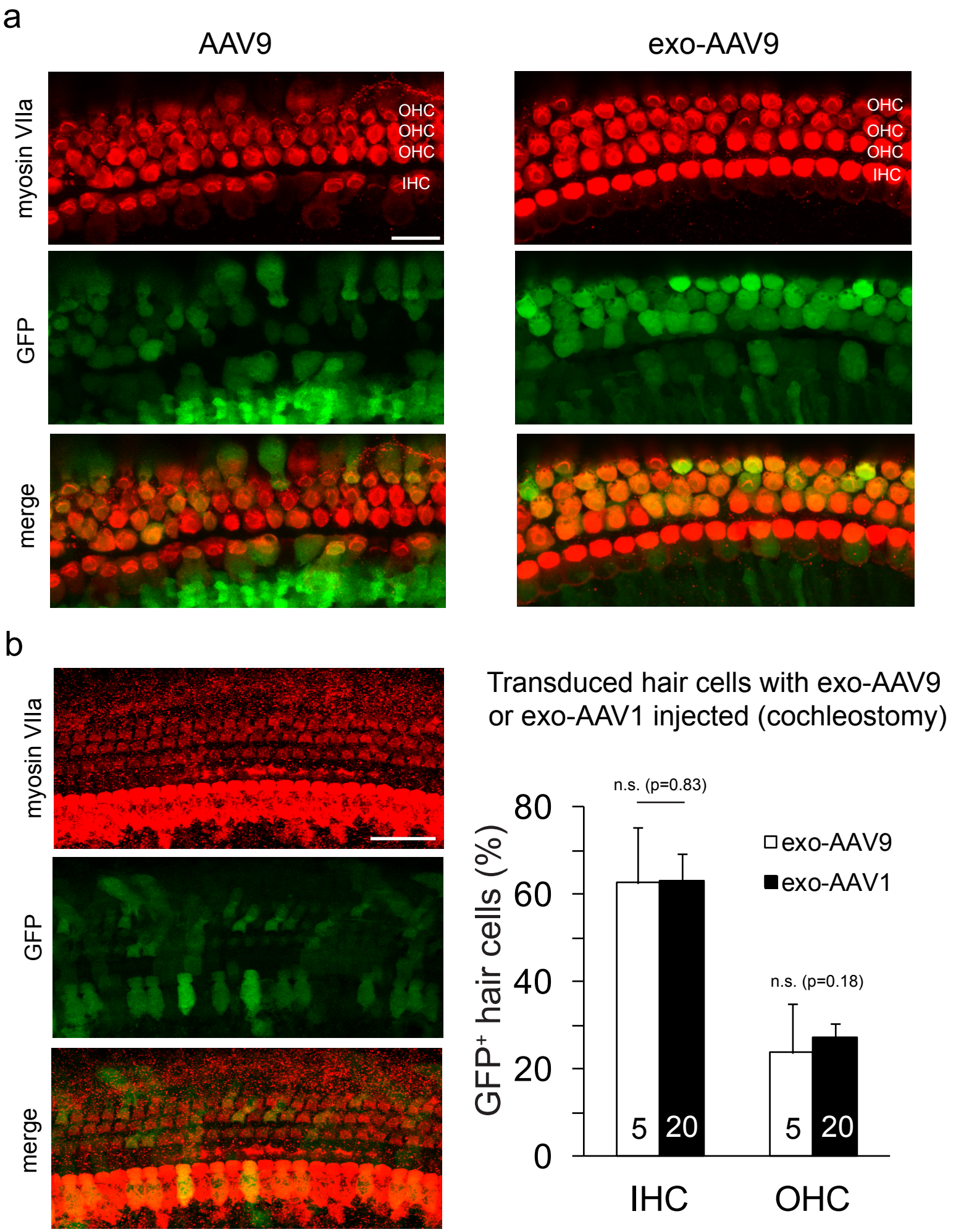
a
AAV9
exo-AAV9
myosin VIIa
GFP
merge
OHC
OHC
OHC
IHC
b
Transduced hair cells with exo-AAV9
or exo-AAV1 injected (cochleostomy)
n.s. (p=0.83)
n.s. (p=0.18)
GFP+ hair cells (%)
80
60
40
20
0
exo-AAV9
exo-AAV1
5
20
5
20
IHC
OHC

Suppl. Fig. 3

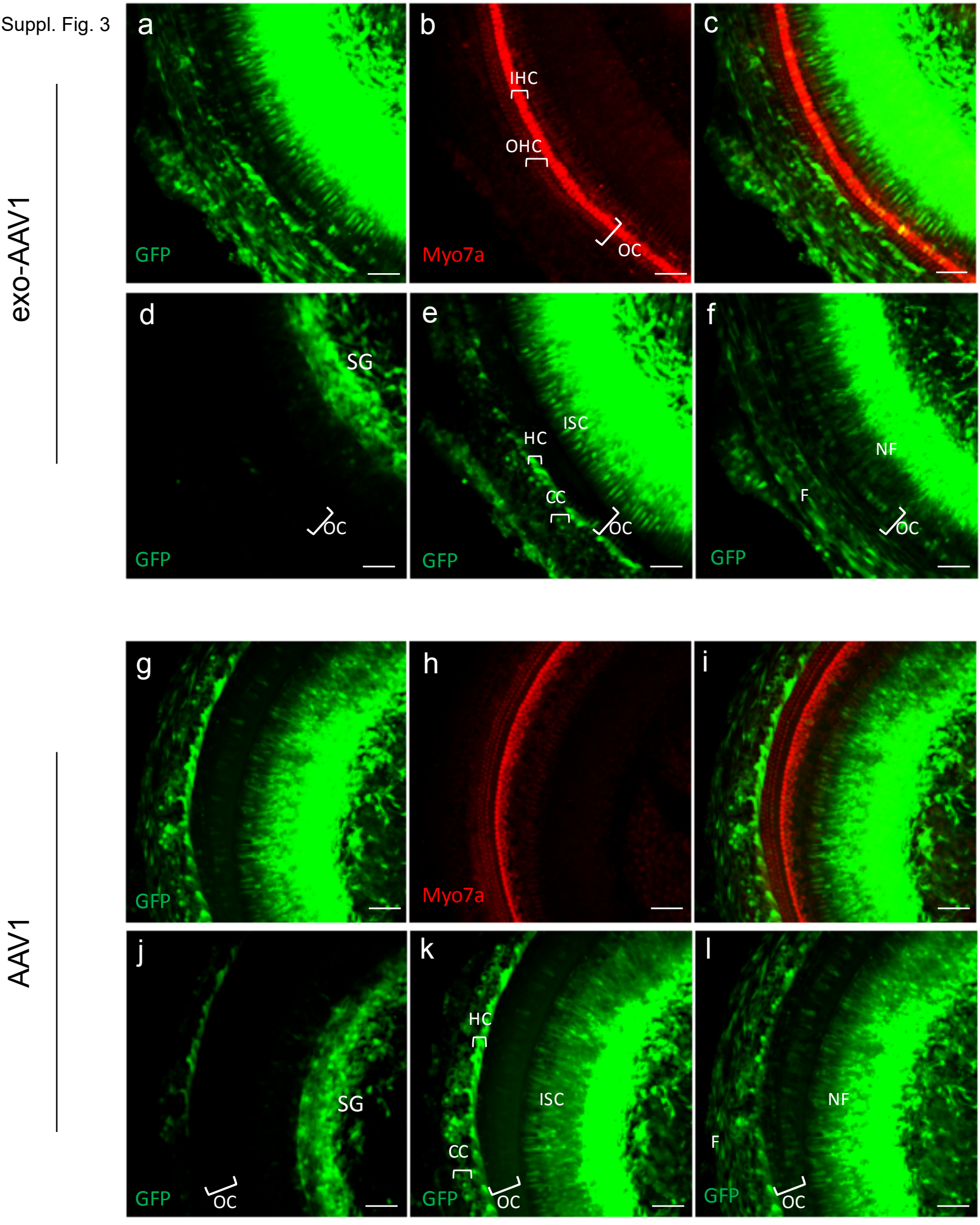
exo-AAV1
AAV1
a
b
c
d
e
f
g
h
i
j
k
l
GFP
Myo7a
IHC
OHC
OC
SG
HC
ISC
CC
NF
F

Suppl Fig 4.

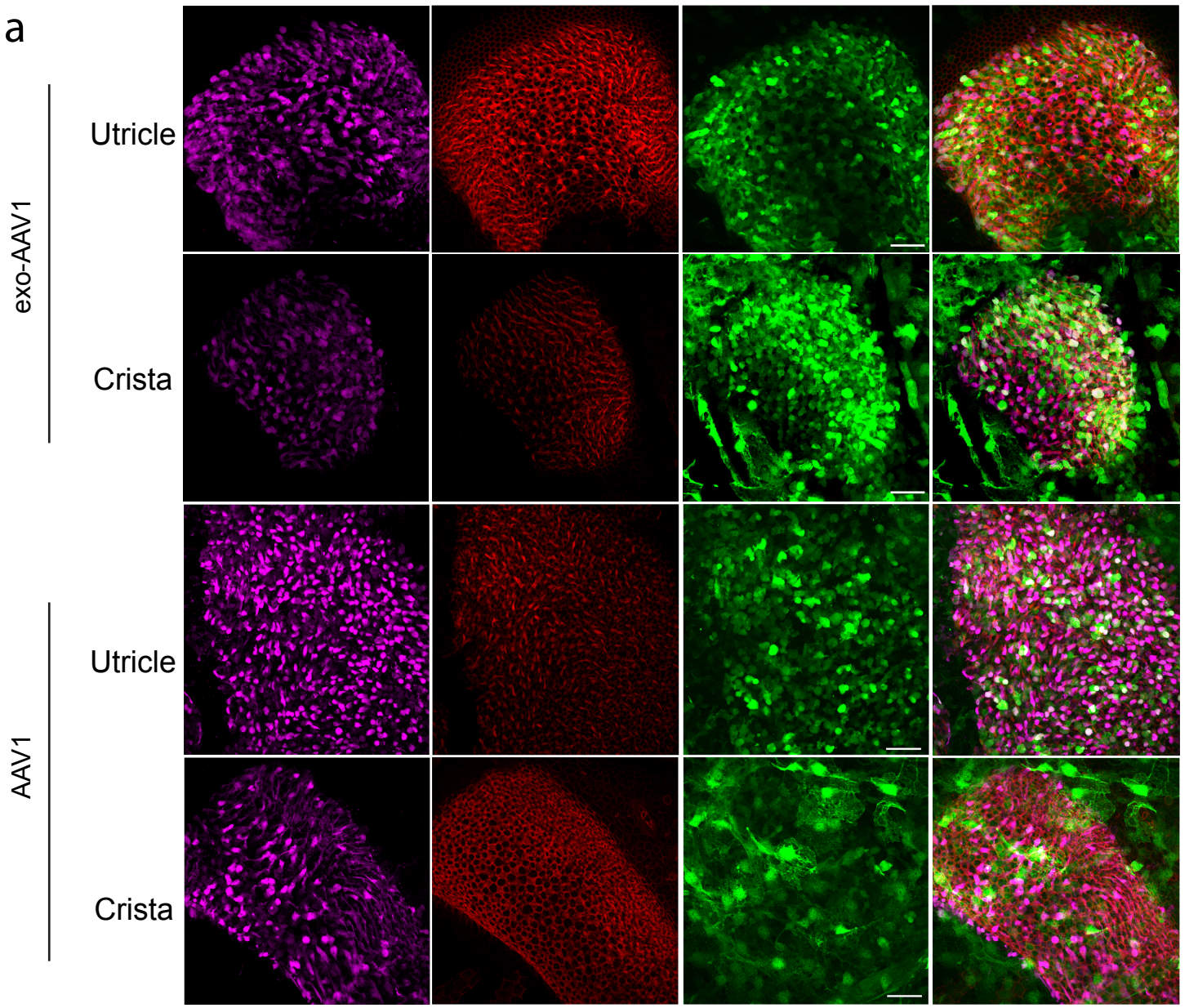
a
exo-AAV1
Utricle
Crista
AAV1
Utricle
Crista

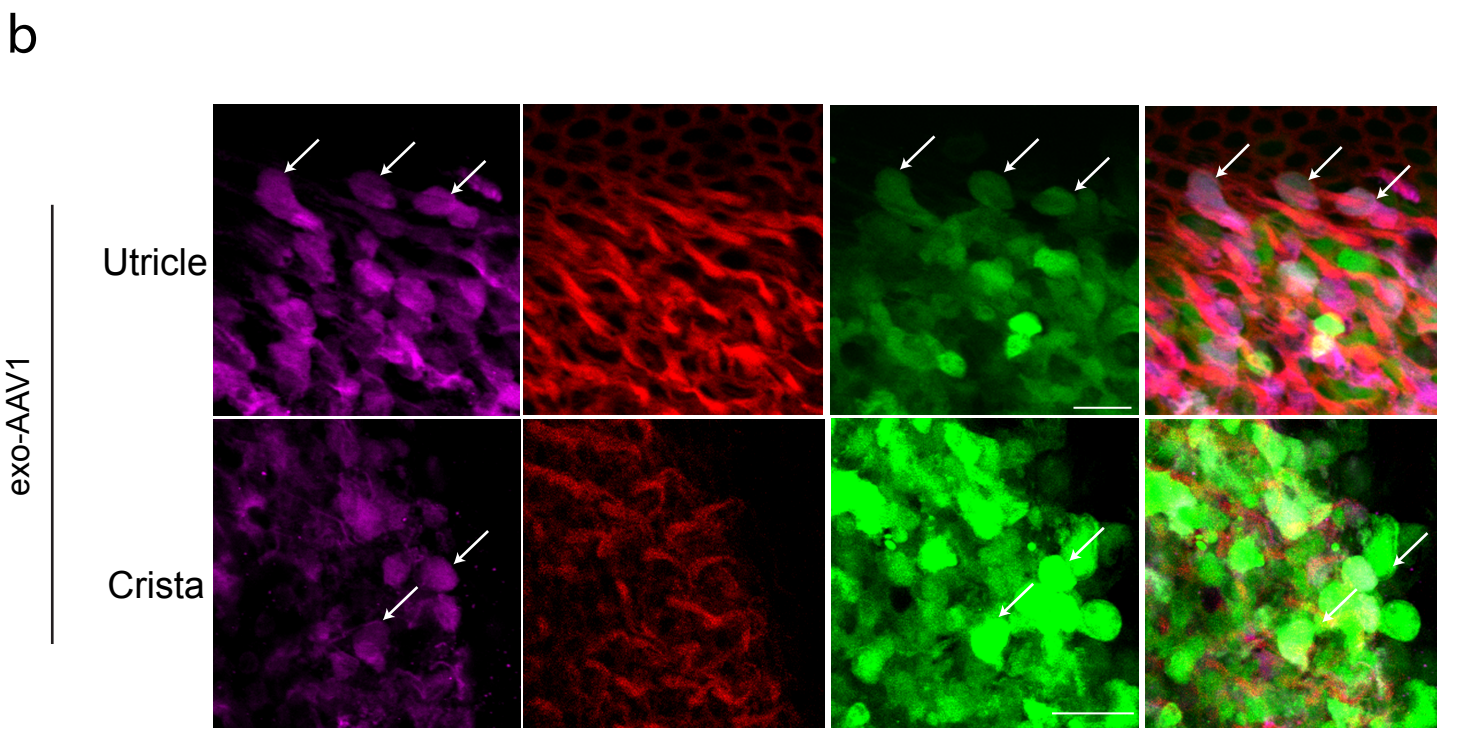
b
exo-AAV1
Utricle
Crista

Suppl. Fig. 5

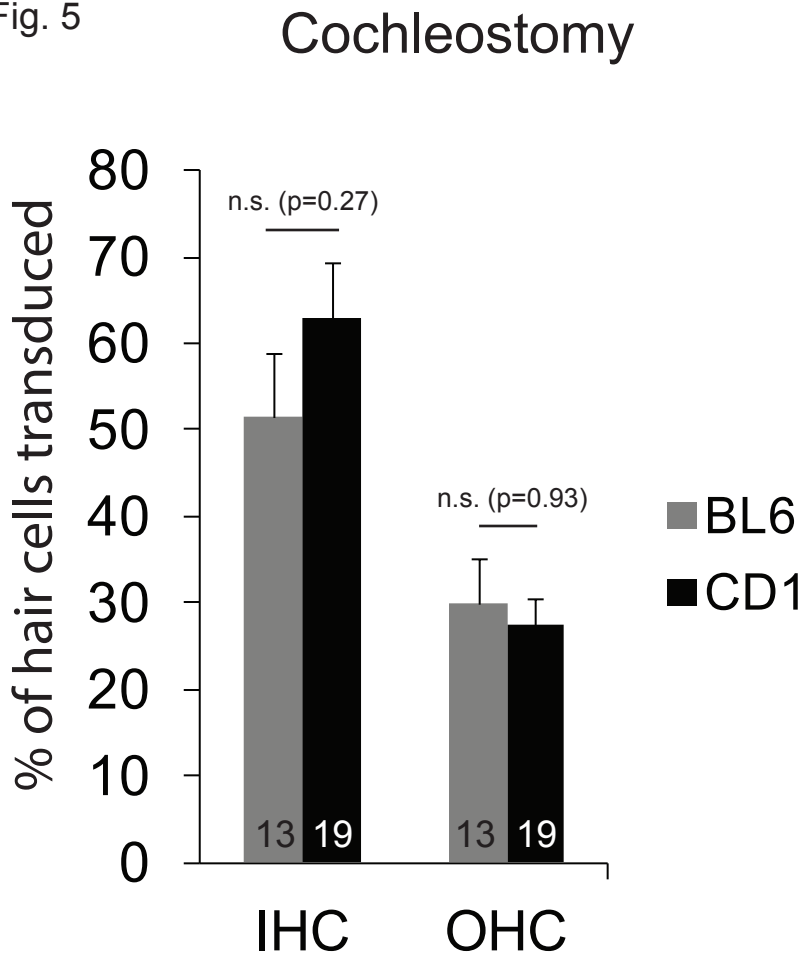
Cochleostomy
% of hair cells transduced
80
70
60
50
40
30
20
10
0
n.s. (p=0.27)
n.s. (p=0.93)
13
19
13
19
IHC
OHC
BL6
CD1

Suppl Fig. 6

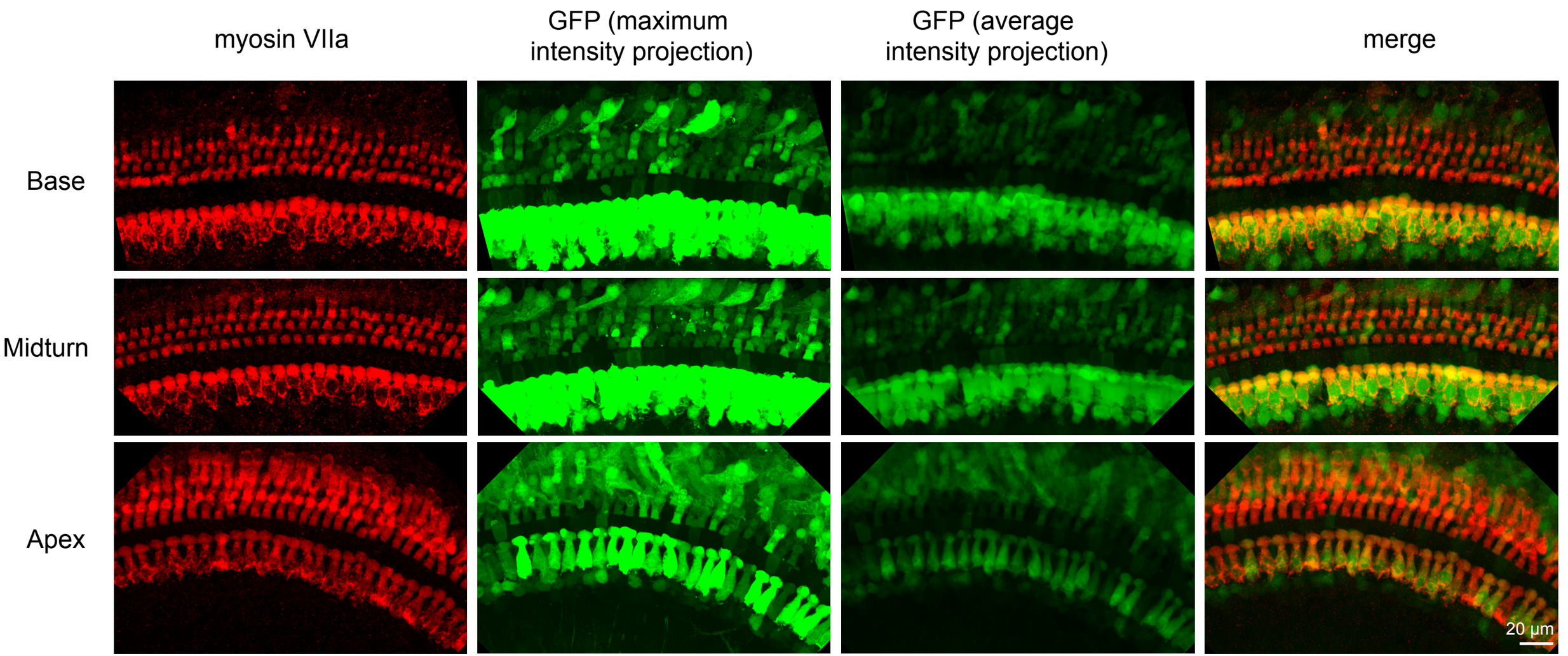
myosin VIIa
GFP (maximum intensity projection)
GFP (average intensity projection)
merge
Base
Midturn
Apex
20 µm

Suppl Fig. 7

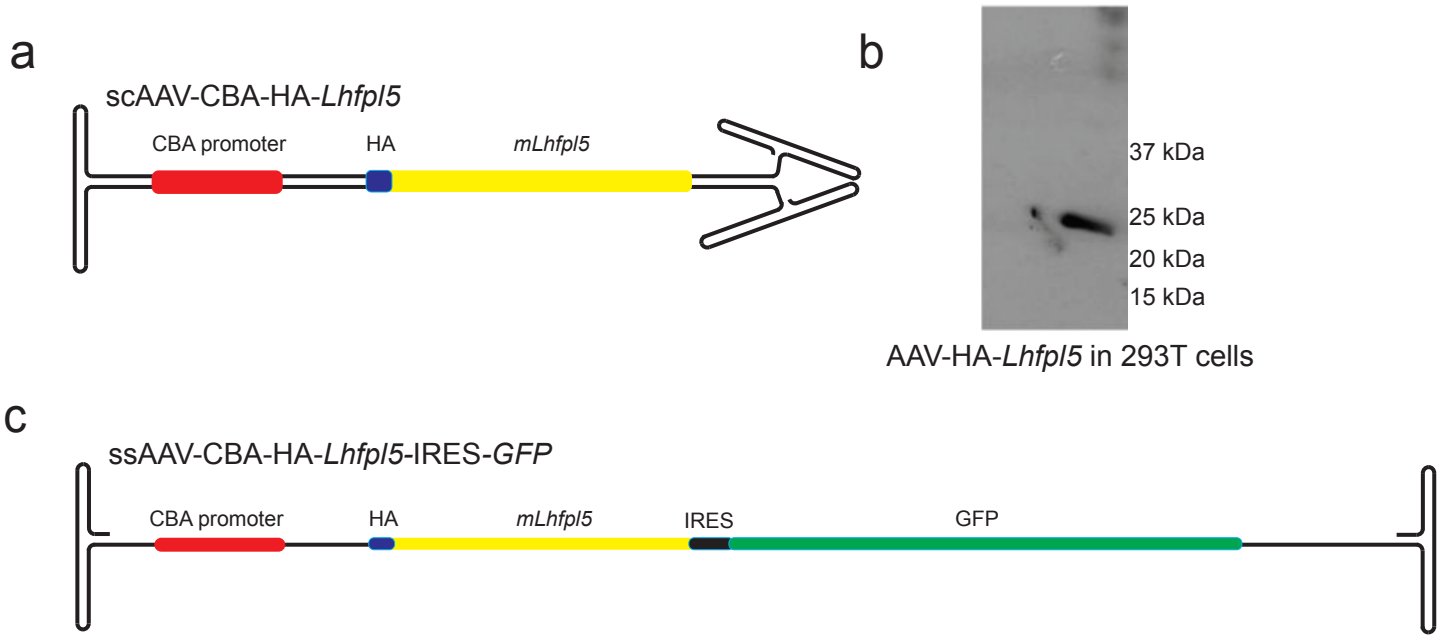
a
scAAV-CBA-HA-*Lhfpl5*
CBA promoter
HA
mLhfpl5
b
37 kDa
25 kDa
20 kDa
15 kDa
AAV-HA-*Lhfpl5* in 293T cells
c
ssAAV-CBA-HA-*Lhfpl5*-IRES-*GFP*
CBA promoter
HA
mLhfpl5
IRES
GFP

Suppl. Fig. 8

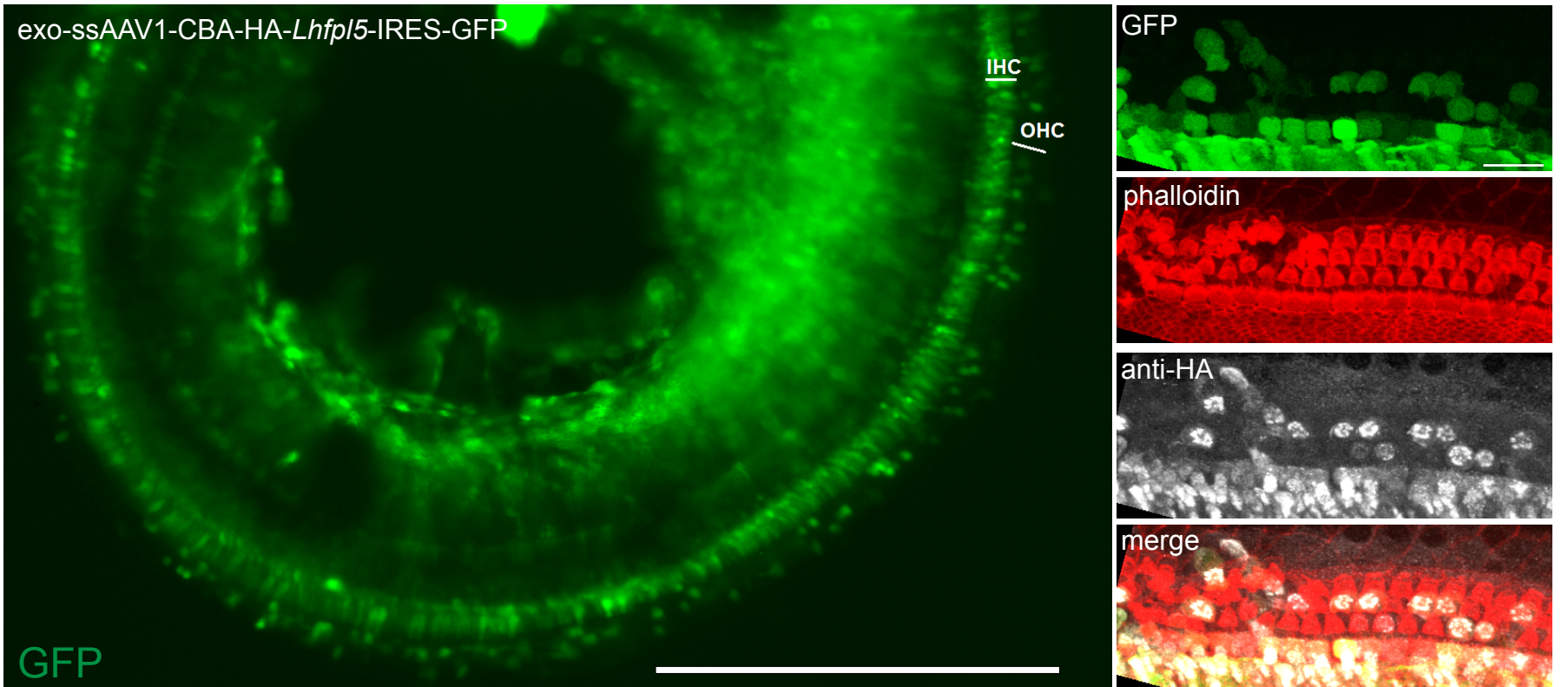
exo-ssAAV1-CBA-HA-*Lhfpl5*-IRES-GFP
IHC
OHC
GFP
GFP
phalloidin
anti-HA
merge

Supplementary Figures and Videos

Supplementary Figure 1. **AAV1 associates with exosomes**. **(a,b)** Cryo-electron microscopy images showing AAV on the surface (a) or the interior (b) of exosomes. Black arrowheads point to exosomal membrane; white arrowheads show AAV capsids on the exterior of the vesicle; white arrows show capsids that appear to be on the interior of the exosome; and black arrow shows one AAV capsid distorting the membrane suggesting it is on the interior of the vesicle. Scale bars are 50 nm. **(c, d)** Transmission electron micrographs of cryosectioned exo-AAV samples that were immunogold-labeled to detect intact AAV1 capsids. AAV capsids are seen on the surface (white arrowheads, c and d) or inside exosomes (white arrow, d). Black arrowheads indicate exosome membrane. Scale bars are 50 nm (c) or 100 nm (d).

Supplementary Figure 2. Exo-AAV9-CBA-GFP outperforms conventional AAV9-CBA-GFP in transduction of cochlear explant hair cells. (a) *In vitro*. Cochleas were explanted from CD1 mice at P1. Vectors were added at $1x10^{11}$ GC the next day for overnight transduction and organs were cultured for three more days. Exo-AAV9-GFP efficiently transduces IHCs and OHCs, labeled with anti-myosin VIIa antibody. Viral transduction is quantified in Fig. 1e. Scale bar is 20 μm. **(b)** *In vivo.* Exo-AAV9 was injected by cochleostomy. The number of hair cells transduced with exo-AAV9 *in vivo* was similar that transduced with exo-AAV1. Scale bar is 30 μm. *Right*, there was no difference between exo-AAV1 and exo-AAV9 in vivo. Exo-AAV1 values are replotted from Fig. 2b for reference. Mean ± SEM.

Supplementary Figure 3. Transduction of cochlear cells by exo-AAV1-GFP and AAV1-GFP vectors administered by cochleostomy. Middle turn of a cochlea at low magnification. CD1 mice were injected at P1, then cochleas were dissected at P14. Hair cells were stained with anti-myosin VIIa antibody (red). **(a-f)** Exo-AAV1. Panels a,d,e,f are confocal images at four different depths. **(g-l)** AAV1**.** Panels g,j,k,l are confocal images at four different depths. For both, other cell types are also efficiently transduced. OC: organ of Corti, IHC: inner hair cell, OHC: outer hair cell, SG: spiral ganglia neurons, ISC: inner sulcus cells, HC: Hensen cells, CC: Claudius cells, NF: nerve fibers, F: fibroblasts. Scale bars: 60 μm.

Supplementary Figure 4. Transduction of the vestibular sensory epithelium by exo-AAV1-GFP and AAV1-GFP vectors, administered by cochleostomy. (a) Low magnification. CD1 mice were injected at P0/P1; the utricle and the ampulla of the lateral semicircular canal were dissected at P14. Hair cells were stained with antibodies to myosin VIIa (purple); actin was labeled with phalloidin (red); and GFP is green. Many vestibular hair cells and supporting cells were transduced, even though the vector was delivered to the cochlea. Scale bars are 30 μm. (b) High magnification. Images show colocalization of GFP with myosin VIIa in hair cells (arrows). Scale bars are 10 μm.

Supplementary Figure 5. Comparison of exo-AAV1-GFP transduction efficiency in CD1 and C57BL/6 mice; injection by cochleostomy. The difference between CD1 (data from Fig. 2b) and C57BL/6 was not significant for either IHCs or OHCs (Mann-Whitney U test). Mean ± SEM.

Supplementary Figure 6. Maximum observed transduction using exo-AAV1 delivered by cochleostomy. C57BL/6 mice were injected by cochleostomy using 0.3 µl of exo-AAV1-CBA-GFP at P1 (resulting in $6x10^9$ GC injected). Cochleas were dissected at P14. Images represent the cochlea with the highest number of GFP-positive hair cells (assessed with direct GFP fluorescence). Scale bar is 20 µm.

Supplementary Figure 7. Schematic of the vectors used in the study. (a) Self-complimentary (sc) AAV-*Lhfpl5* constructs. We synthesized a mouse codon-optimized AAV expression cassette containing a hemagglutinin (HA) tag on the N-terminus. Expression was driven by the chicken beta-actin (CBA) promoter. **(b)** Western blot of protein from AAV-producer 293T cells using anti-HA. LHFPL5 protein has a molecular weight of 24 kDa. **(c)** Schematic of the single stranded (ss) AAV-CBA-*HA-Lhfpl5*-IRES-*GFP* construct. IRES: internal ribosomal entry site.

Supplementary Figure 8. Co-expression of GFP and HA-LHFPL5 after i*n vivo* injection of exo-AAV-CBA-*HA-Lhfpl5*-IRES-*GFP*. *Lhfpl5*$^{-/-}$ mice (C57BL/6 background) were injected through the round window at P1 and cochleas were dissected at P6. The single-stranded construct transduced IHCs and OHCs, revealed by GFP expression. Furthermore, GFP-positive cells showed anti-HA labeling in the cell body and in the bundle, confirming the correlation between GFP expression and LHFPL5 localization in bundles. Scale bars are 400 µm (left panel) and 20 µm (right panel).

Supplementary Video 1. Startle response. *Lhfpl5*$^{+/-}$, *Lhfpl5*$^{-/-}$, and *Lhfpl5*$^{-/-}$ animals injected with exo-AAV1-CBA-*Lhfpl5* were placed in an opaque white bucket and allowed to equilibrate for several minutes in quiet. An investigator performed a hand clap, which was not visible to the animals. Animals that can hear the clap momentarily freeze (Preyer reflex).

Supplementary Video 2. Open field test. *Lhfpl5*$^{+/-}$, *Lhfpl5*$^{-/-}$, and *Lhfpl5*$^{-/-}$ animals injected with exo-AAV1-CBA-*Lhfpl5* were placed in an opaque white arena. Normal mice explore the new environment and show head and gait stability. *Lhfpl5*$^{-/-}$ animals show head tossing, gait instability, circling and backward movement.